EB2020-STP-056

Identification and Classification of Nonlinear Stick-Slip Phenomena on Complex Disk Brake Systems

Aleš Belšak[1], Jurij Prezelj[2], Severin Huemer-Kals[3], Karl Häsler[4]

[1]*University of Maribor, Faculty of Mechanical Engineering, Smetanova 17, 2000 Maribor, Slovenia (E-mail:ales.belsak@um.si)*
[3]*University of Ljubljana, Faculty of Mechanical Engineering, Aškerčeva cesta 6, 1000 Ljubljana, Slovenia*
[2]*Graz University of Technology, Institute of Automotive Engineering, Inffeldgasse 11/II, 8010 Graz, Austria*
[4]*Mercedes-Benz AG, 71059 Sindelfingen, Germany*

https://doi.org/10.46720/EB2020-STP-056

ABSTRACT: Disk brake creep groan is a noise and vibration phenomenon generated by stick-slip during braking at slow vehicle speeds and low brake pressures. These operational states are especially present with automatic transmissions, automated driving functions and quiet, electrified drivetrains, which favor occurrence and also perception of creep groan vibrations. Creep groan phenomena lower the impression of a vehicle's quality and can even be mistaken for a damaged brake system. To investigate and tackle such problems, real time identification of creep groan phenomena is needed. Therefore, an approach based on Quasi Acoustic Emission measurements is presented. This approach utilizes the character of stick-slip transitions: Due to a stick-slip transition's inherent abrupt force change, vibrations with energy distribution over a wide frequency range occur. By subsequently applying a high-pass filter, a squaring, an amplification and a low-pass filter, a vast number of measured creep groan vibration signals was transformed into new, refined signals. New features were extracted from these signals and analyzed by a *k*-means algorithm. Results show that these Quasi Acoustic Emission features provide promising information for the automatic identification of creep groan in real time.

KEY WORDS: Automatic Classification, Brake NVH, Creep Groan, *K*-Means Algorithm, Signal Features, System Identification, Vibroacoustics

1. Introduction

Creep groan phenomena occur during braking at low speeds and during slow acceleration to and from standstill, [1, 2]. High level of vibration and noise can result, with both being unpleasant and often unacceptable for the passenger. To reduce related warranty costs, the automotive industry is looking for solutions to overcome this problem. Hence, many studies have been performed to understand the behavior of creep groan phenomena in recent years, see e.g. [3, 4, 5, 6, 7, 8, 9, 10].

Stick-slip transitions were found to be inherent to creep groan phenomena, although new studies also propose influences from vibro-impact [6, 11]. A study based on different minimal models within [5] has shown that stick-slip vibrations occur in strong interaction with the underlying frictional behavior and the structure of the mechanical response system. On one hand, stick-slip transitions can excite a mechanical response system. On the other hand, the mechanical response system can be seen as a feedback loop, acting on the stick-slip transitions and their frequencies itself.

Stick-slip is a nonlinear physical phenomenon comprising of abrupt phase transitions of relative velocity; from zero to a finite relative velocity. Due to these virtually instantaneous changes in velocity, the accelerations and consequent forces acting on a response system have the shape of impulses. The energy of a single stick-slip is therefore distributed across a wide frequency range: from a few Hz up to some tens of kHz. Within [5], these stick-slip impulses are explained to be similar to step functions, indicating the low-frequency characteristic of creep groan.

Mechanical response systems, as in creep groan's case at least the vehicle's brake and axle system, respond to excitations with movement. This resulting movement re-affects the characteristic and occurrence of the stick-slip vibrations. The repetition frequency of stick-slip transitions is therefore inherently shifted into the frequency range of the mechanical response system. Simulations have been performed in order to confirm the understanding of the mechanism, see e.g. [12]. The length of a stick-slip impulse and (consequently) the high-frequency content in the vibration signal were evaluated.

It turns out that in typical brake systems of passenger cars, creep groan appears in two classes: Low-frequency creep groan from 10 – 30 Hz as well as high-frequency creep groan from 40 – 100 Hz, [2, 12, 13]. The mechanism of low-frequency groan from 10 – 30 Hz is highly impulsive and rather "hard" with distinct stick phases, superposed by high-frequency vibrations. In some applications, this low-frequency groan may be shifted to higher required brake pressures, explaining why this is probably neither detected nor considered a problem, see e.g. [2]. The "soft", high-frequency creep groan in the range of 40 – 100 Hz shows characteristics more similar to harmonic-like vibrations. This type of creep groan was found to occur at rather low brake pressures which are relevant for practical vehicle operating conditions, [2].

For creep groan identification, experimental studies such as [2] often utilize tools in frequency domain. These tools typically focus on the main creep groan frequency and the occurrence of higher harmonics. Unfortunately, increasing the resolution in frequency domain means blurring short-time events and vice versa. These

fundamental relations between frequency and time domain complicate a clear detection of creep groan in time domain and are therefore one argument to study time-based detection approaches as explained within this work.

2. Signal Analysis and Feature Extraction

2.1. Quasi Acoustic Emission

Acoustic Emission (AE) is the emission of elastic stress waves caused by deformation and fracture of materials. Simply put, AE is the voice of the materials. By listening to the AE, one can extract processes that are occurring in the material or on the contact surface between two parts. In tribological processes, AE waves are generated by deformation and fracture of contacting surfaces. By measuring AE signals during tribological processes, valuable information can be obtained: Within [14], various friction and wear tests were carried out to clarify their interrelationships. It was found that the sound emission generated by sliding friction (slip event) can be detected in the frequency range from 2 kHz to 100 kHz, [14]. C. Ferrer et al., [15], published a research paper using the AE technique to record and study the elastic waves occurring at the transition from static to kinetic friction in a stick-slip experiment with a soft steel sheet and a quenched steel clamp. They found that the beginning of the slip event was accompanied by an increase in continuous AE activity and immediately thereafter by a long AE wave train. They identified the main characteristic of these trains to have a typical sequence defined by a first wave with a relatively low amplitude and the very high amplitude of the three or four next trains. Afterwards the wave train amplitudes decay, [15]. The results presented by Ferrer et al. [15] and Stoica [16] suggest that a single stick-slip effect is accompanied by a train of AE bursts. Individual bursts of AE are shorter than 30 ms: However, the AE burst trains last much longer than 30 ms and always start with a low amplitude wave. According to the results of Ferrer and Stoica, the total duration of the stick-slip transition in the form of AE bursts echoes up to 10 ms, i.e. in the frequency range around 100 Hz, similar to the 1st order frequency of creep groan.

This observation led to the idea to design an analysis of vibration signals in the frequency range above 2 kHz and to observe impulses in the vibration signal correlating to trains of AEs. Since vibration sensors in the AE range do not have an appropriate response, this approach is referred to as Quasi Acoustic Emission (QAE) (Figure 1, 2).

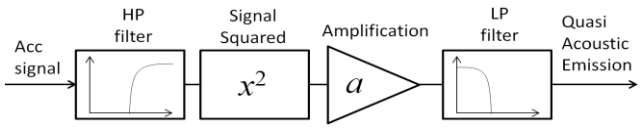

Figure 1 Processing of a vibration signal for the extraction of features based on Quasi Acoustic Emission (QAE)

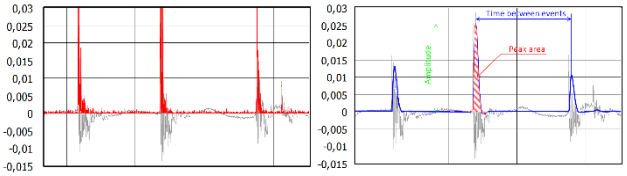

Figure 2 Transformation of a creep groan vibration signal into a Quasi Acoustic Emission (QAE) signal for further feature extraction

The aim of signal processing was to transform the high-frequency content within the vibration signal to refined pulses. The coefficient of amplification depends on the difference between the cutoff frequency of the high-pass and the cutoff frequency of the low-pass filter. In the present case, the amplification was set according to the equation (1):

$$a = \pi^2 \left(\frac{f_{HP}}{f_{LP}} \right) \tag{1}$$

High-frequency content is correlated to the stick-slip occurrence. The additional low-pass filter is used to reshape the squared signal into clear peaks. This enables to count the pulses, with pulse maxima located virtually exactly in time with stick-slip occurrence. By this, time between stick-slip occurrences as well as pulse amplitudes can be measured.

2.2. *K*-Means Algorithm

The *k*-means algorithm is one of the most common unsupervised clustering algorithms [17, 18]. *K*-means is an iterative algorithm aiming to classify a given dataset into *K* distinct non-overlapping clusters, where each data point belongs to one group only. Data points are *D*-dimensional vectors where each component represents an extracted feature from observations. The *k*-means algorithm tries to arrange *N* observations into *K* clusters in a way where inter-cluster data points are as similar as possible while keeping the clusters as far as possible. The evaluation of similarity between points is based on the Cartesian distance between points. The distance between a centroid c_m and the observed point x_n is defined by the equation (2):

$$\left| \mathbf{c}_m \mathbf{x}_n \right|^2 = \sum_{i=1}^{D} c_{m,i}^2 - x_{n,i}^2 \tag{2}$$

The *k*-means algorithm assigns each data point to the closest cluster, defined by its centroid. The algorithm is based on minimization of the arithmetic mean of all the data points that belong to the same cluster. The less variation is within the clusters, the more homogeneous the data points are within each cluster. *K*-means clustering therefore aims to classify the *N* observations into *K* ($\leq N$) clusters defined by centroids $C = \{c_1, c_2 \ldots c_k\}$ in a way to minimize the within-cluster sum of squares. Formally, the objective is to find:

$$\underbrace{\operatorname{argmin}}_{\mathbf{C}} \sum_{i=1}^{K} \sum_{x \in \mathbf{c}_i} \left\| \mathbf{x}_i - \varepsilon_i \right\|^2 = \underbrace{\operatorname{argmin}}_{\mathbf{C}} \sum_{i=1}^{k} \left| \mathbf{c}_i \right| Var \mathbf{c}_i \tag{3}$$

where ε_i is the average of points attributed to $\mathbf{c}_i$. This is equivalent to minimizing the pairwise squared deviations of points in the same cluster:

$$\underbrace{\arg\min}_{\mathbf{C}} \sum_{i=1}^{K} \frac{1}{|2\mathbf{c}_i|} \sum_{\mathbf{x},\mathbf{y}\in\mathbf{c}_i} \|\mathbf{x}-\mathbf{y}\|^2 \quad (4)$$

The equivalence can be deduced from identity:

$$\sum_{\mathbf{x}\in\mathbf{c}_i}^{k} \|\mathbf{x}-\boldsymbol{\varepsilon}\|^2 = \sum_{\mathbf{x}\neq\mathbf{y}\in\mathbf{c}_i} (\mathbf{x}-\boldsymbol{\varepsilon}_i)(\boldsymbol{\varepsilon}_i-\mathbf{y}) \quad (5)$$

Because the total variance is constant, this is equivalent to maximizing the sum of squared deviations between points in different clusters, which follows from the law of total variance.

The *k*-means algorithm is usually initiated with a matrix of centroids *C* filled with random numbers. Then Cartesian distances are calculated for each pair of data points to each centroid representing one class. Each data point is then attributed to the class to which its centroid distance is minimal. New centroids are then calculated from a new distribution of data points for each class; the new centroid of a given class is an averaged value of all data points attributed to this class. Cartesian distances are calculated once again and the process continues until no more transitions of data points between classes happen.

3. Experimental Plan

Creep groan was measured on a complete vehicle system to create a data basis for the development of an identification and classification method. Different driving parameters were selected with the aim to create creep groan vibrations. These parameters included different combinations of driving direction (forward or backward), acceleration (acceleration from or to a standstill) and inclination of the road (15% hill or flat track). A series-production compact executive car with an automatic transmission was selected.

Accelerometers were mounted on the brake caliper carriers of the front axle, as shown in Figure 3. Signals from these 3D-accelerometers were recorded with a sampling frequency of 51200 Hz, .wav-files with an amplitude resolution of 16-bit were created. Although 3D-accelerometers were used and signals from all orientations were recorded, it was found that the most prominent direction is perpendicular to the mounting plane as indicated in Figure 3 – this relates mostly to the vertical caliper carrier acceleration.

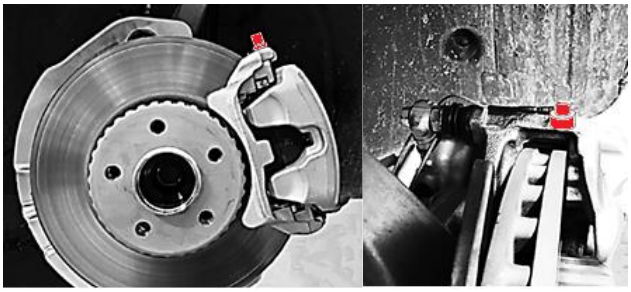

Accelerometer :
Sensitivity (±15%) = 10 mV /g
Resonance frequency ≥ 45 kHz
Frequency range ± 5%; 1Hz-9kHz
Frequency range ±10%; 0,5H -12kHz

Figure 3 Placement of accelerometers

During the analysis, signals were retrieved from the .wav-files and arranged in 125 ms long sequences. All signal processing was performed using *NI LabVIEW 16*. Separate programs have been prepared for QAE signal processing, peak detection, peak counting, measuring time between peaks and for peak surface integration. The *k*-Means Algorithm was prepared in *NI LabVIEW 16* as well.

4. Results and Discussion

Extracting QAE pulses from acceleration signals was performed by the proposed approach consisting of filtering, amplification and squaring. For the high-pass and low-pass filters, 2nd order Butterworth IIR-filters were selected. Three parameters of data processing were left to be optimized: high-pass filter cutoff frequency, amplification and low-pass filter cutoff frequency.

At first, the high-pass filter cutoff frequency was chosen at 16 kHz by trial and error. The amplification factor was chosen according to equation (1) analogously.

Eventually, low-pass cutoff frequency was found to have a large impact on the shape of the peaks: A lower low-pass cutoff frequency (160 Hz in Figure 4 left) provides peaks with smooth shape. This smooth shape is favorable for the peak detection algorithm, however, it blurs the boundary between two close neighboring peaks. Higher values of low-pass filter cutoff frequency (500 Hz in Figure 4 right) provide rather sharp peaks, which closely follow the stick-slip event. Unfortunately, the low-pass filter cutoff frequency cannot be increased significantly above 500 Hz, due to the occurrence of 'ghost' peaks, which result from splitting one peak. All further results are therefore based on QAE obtained with a low-pass filter cutoff at 500 Hz, as shown in Figure 4 right.

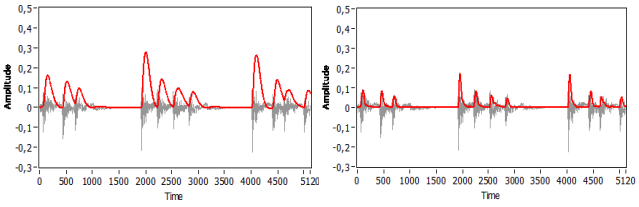

High-pass filter cutoff freq. = 16 kHz
Low-pass filter cutoff freq. = 160 Hz

High-pass filter cutoff freq. = 16 kHz
Low-pass filter cutoff freq. = 500 Hz

Figure 4 The influence of the applied filters cutoff frequencies on the results of acceleration signal processing to mimic the QAE

Identifying impulses generated by stick-slip effect enables measuring the time difference between two successive impulses. Furthermore, the released energy of individual stick-slip transitions can be estimated by measuring height and surface area below the peak. Different modes of creep groan are presented in Figure 5.

One second of a typical creep groan vibration signal is presented in Figure 5; separated in eight sections of 125 ms $t_1 - t_8$. The detected time between peaks of QAE is presented directly below, in the form of discrete frequency. This blue curve shows changes of the discrete frequency extracted directly from time difference between two peaks. Changes in discrete frequency between base frequency

and higher values indicate that during basic frequency of stick-slip occurrence, another event is inserted, as shown in example t_2 and t_3 on the Figure 5.

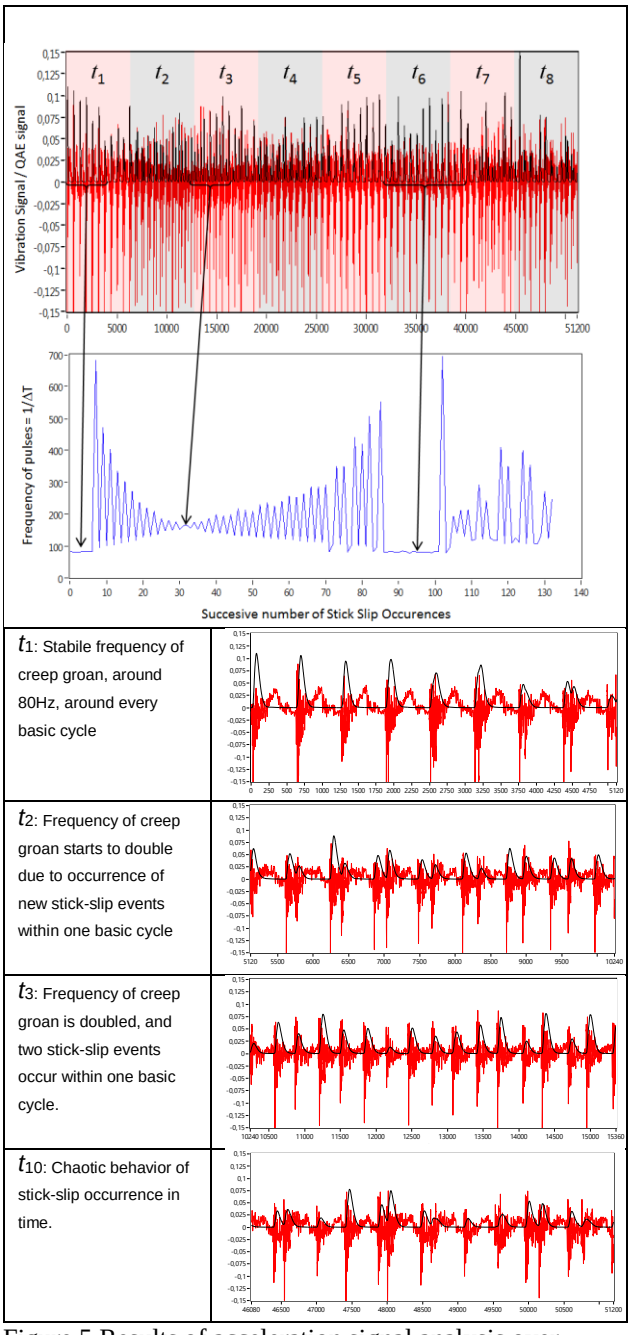

Figure 5 Results of acceleration signal analysis over time [s] based on QAE approach for example signal I.

From the acceleration signal, the following features based on QAE were extracted for each 125 ms long interval:

- the number of stick-slip transitions,
- the maximum pulse height,
- the average height of the pulse,
- the relative standard deviation of the height of pulses,
- the frequency of the pulses,
- the relative standard deviation of the frequency of pulses,
- the area under the pulses,
- RMS of the vibration signal for frequencies < 250 Hz,
- RMS of the vibration signal for frequencies > 16 kHz,
- RMS of the vibration signal.

40 measurements were included into the statistical analysis. Recorded signals were of different lengths. For the feature extraction, all results were merged into a single matrix containing 8500 feature vectors. For the identification of the proper number of classes, the convergence of the initial randomly generated centroid matrix was observed. The probability of the *k*-means optimization's convergence based on randomized initial centroids was evaluated for a different number of classes. It was found that, by increasing the number of classes, the probability of the algorithm to converge is reduced, as it is shown in Figure 6.

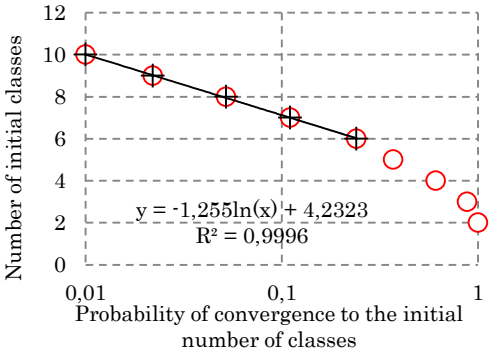

Figure 6 Relation between the number of predefined initial classes and the probability of the *k*-means algorithm converging to all the predefined classes.

Furthermore, it can be observed that the number of classes is almost perfectly correlated to the logarithm of the convergence probability for a higher number of classes. When the number of initial classes is reduced, the probability of convergence stops following the interpolated curve. In our case, this occurred at a number of approx. 5 classes, leading towards the assumption that the present data set can be classified well into 5 classes. One of the classes is reserved for standstill/no occurrence of creep groan whereas the other 4 classes are reserved for different types of creep groan. Table 1 shows an overview of centroid values for the 5 different classes A-E.

Table 1 Centroids for five creep groan classes classified by *k*-means algorithm

	CLASS				
Extracted signal features	**A**	**B**	**C**	**D**	**E**
Number of detected pulses	0	0	0,210	0,520	0,844
Max of QAE Pulse height	0	0	0,143	0,155	0,09
Log (AVG of QAE pulse height)	0	0	0,169	0,146	0,107
RSD of QAE pulse height	0	0	0,164	0,244	0,097
AVG frequency of QAE pulses	0	0	0,183	0,436	0,591
STD frequency of QAE pulses	0	0	0,011	0,656	0,073
Log (Area under QAE pulses)	0,012	0,087	0,502	0,576	0,629
Log (RMS in LFR < 250Hz)	0,141	0,476	0,518	0,665	0,798
Log (RMS in HFR > 16kHz)	0,019	0,117	0,465	0,532	0,583
Log (RMS)	0,131	0,514	0,695	0,805	0,886

Figure 7 presents centroids of the amplitude of vibration signals for three different frequency ranges: The low-frequency range < 250 Hz, the high-frequency range > 16 kHz and the full frequ. range. For different features extracted from the vibration signal based on QAE signal processing, centroids are shown in Figure 8.

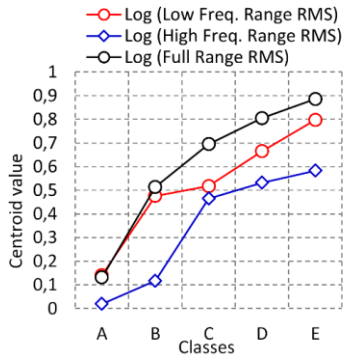

Figure 7 *K*-means class centroid values of investigated vibration signals for three different frequency ranges: < 250 Hz, >16 kHz and full frequ. range.

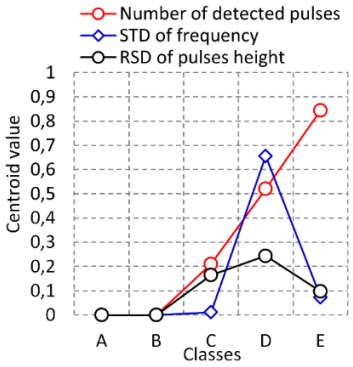

Figure 8 *K*-means class centroid values of different features extracted from the vibration signals by QAE.

The analysis of converged centroids clearly shows that class A represents the part of the vibration signal where no activity is present. Class B is defined by vibrations with no distinct stick-slip pulses. Class B can be related to an increased level of (harmonic) vibrations in the low-frequency range below 250 Hz.

Classes C, D and E are predominantly defined by a certain number of detected QAE pulses and can therefore be considered as “real” creep groan classes.

Class C is defined by 2 QAE occurrences of pulses within the 125 ms long interval. Class C intervals show a high level of vibrations in the high-frequency range and a relatively low level of vibrations in the low-frequency range. This can be related to single or a low number of subsequent stick-slip transitions.

Class D is predominantly defined by at least 4 and up to 8 QAE occurrences of pulses within the 125 ms long interval. Class D contains high-level vibration signals, both in low- and high-frequency range.

Class E is defined by a fully developed creep groan with at least 8 detected pulses within the 125 ms long interval; combined with small deviations of the time intervals between QAE pulses. Vibration levels of all three frequency ranges are highest for creep groan in class E. For the investigated vehicle, such behavior corresponds to frequency peaks between 72 and 88 Hz in the vibration signal frequency spectrum. A classification example based on 5 extracted features is given in Figure 9.

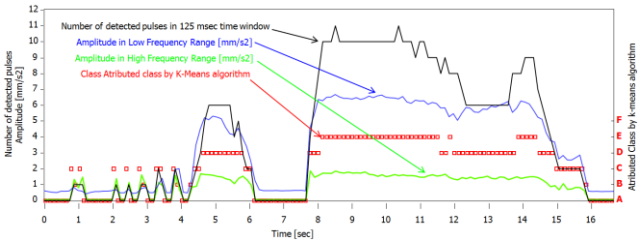

Figure 9 The classification of the acceleration signal based on selected features within 125 ms time intervals for example sequence II.

In industry, a vehicle’s creep groan behavior is usually assessed subjectively. During such a subjective assessment, trained test drivers listen to the creep groan noise and feel the vibrations. Due to creep groan’s high sensitivity towards parameters such as brake pressure and vehicle speed, different modes of creep groan can occur during practical tests. Hence, test drivers often have to rate different modes of creep groan within one test – a difficult task.

Based on the presented evaluation of creep groan classes, this task could be performed objectively e.g. for recordings of 8 s as within Figure 10 and Figure 11: Again, classes were attributed to each time window of a length of 125 ms. The relative occurrence of each class can then be used as a base for further rating algorithms, considering not only general creep groan occurrence but also the type of creep groan.

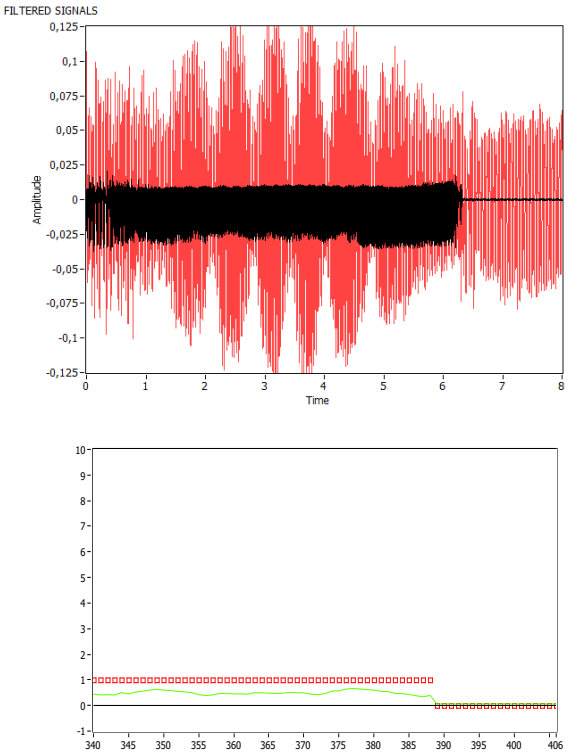

Occurrence of Class A: 15
Occurrence of Class B: 0
Occurrence of Class C: 49
Occurrence of Class D: 0
Occurrence of Class E: 0

Figure 10 Types of creep groan classified based on the *K*-means algorithm for example sequence III.

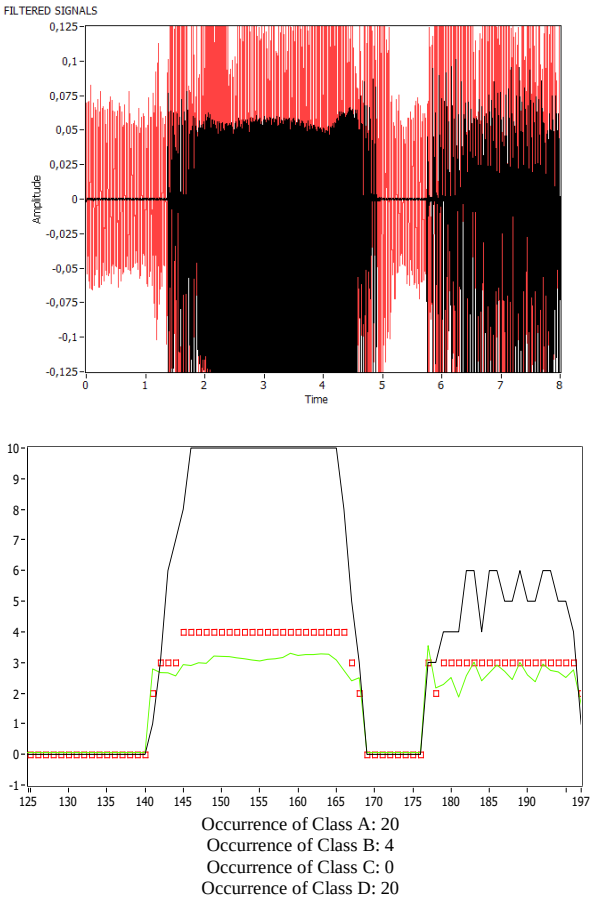

Occurrence of Class A: 20
Occurrence of Class B: 4
Occurrence of Class C: 0
Occurrence of Class D: 20
Occurrence of Class E: 2

Figure 11 Types of creep groan classified based on the *k*-means algorithm for example sequence IV.

5. Conclusion

Brake caliper acceleration signals obtained during creep groan phenomena have energy in a wide frequency range from a few Hz up to more than 20 kHz due to the occurrence of stick-slip vibrations. From previous studies it is known that Acoustic Emission (AE) generated by the stick-slip effect contributes to the energy of a vibration signal in the frequency range above 5 kHz. Based on an acceleration signal transformed by intelligent filtering, scaling and squaring, a new method called Quasi Acoustic Emission (QAE) can be introduced. By extracting vibration signal features from this QAE, excellent input data is obtained for the unsupervised clustering algorithm *k*-means.

For a given dataset of complete vehicle creep groan measurements, the *k*-means algorithm identified five different vibration classes based on QAE features; three of them containing different kinds of stick-slip related creep groan.

In case of the creep groan classes, the time between stick-slip occurrences proved to be the most important feature for classification. It corresponds to the base frequency of creep groan.

The second most important feature for classification was found to be the standard deviation of time intervals between QAE peaks, indicating the stability of the creep groan phenomenon.

The third most important features for classification are the effective values of the investigated acceleration signal for low-frequency range (< 250 Hz) as well as for the high-frequency range (> 16 kHz).

Eventually, the presented algorithm shows an effective and practicable tool for detecting and classifying creep groan based on objectively measured acceleration data. Further potential of the method could lie in the application on simulation data.

References

[1] Brecht, J.: Untersuchungen zum Bremsenknarzen. Ein Beitrag zur Beschreibung von Schwingungen in Bremssystemen. Also: Universität Siegen, Dissertation, 2000. Berichte aus der Fahrzeugtechnik. Shaker, Aachen (2000)

[2] Pürscher, M., Fischer, P.: Systematic Experimental Creep Groan Characterization Using a Suspension and Brake Test Rig. SAE Technical Papers (2017). https://doi.org/10.4271/2017-01-2488

[3] Abdelhamid, M.K.: Creep groan of disc brakes. SAE Technical Papers (1995). https://doi.org/10.4271/951282

[4].Brecht, J., Hoffrichter, W., Dohle, A.: Mechanisms of brake creep groan. SAE Technical Papers (1997). https://doi.org/10.4271/973026

[5] Marschner, H., Leibolt, P., Pfaff, A., Morschel, C.: Untersuchung der Wirkmechanismen reiberregter Haft-

Gleit-Schwingungen am Beispiel des Bremsenknarzens und analoger Schwingungsphänomene. In: Breuer, B. (ed.) XXXV. Internationales µ-Symposium - Bremsen-Fachtagung. Bad Neuenahr, Oct 28-29, pp. 84–104. VDI-Verlag, Düsseldorf (2016)

[6] Meng, D., Zhang, L., Xu, X., Sardahi, Y., Chen, G.S.: Sensing and quantifying a new mechanism for vehicle brake creep groan. Shock and Vibration (2019). https://doi.org/10.1155/2019/1843205

[7] Zhao, X., Gräbner, N., von Wagner, U.: Theoretical and experimental investigations of the bifurcation behavior of creep groan of automotive disk brakes. Journal of Theoretical and Applied Mechanics (Poland) (2018). https://doi.org/10.15632/jtam-pl.56.2.351

[8] Zhao, X., Gräbner, N., Wagner, U., Hetzler, H.: Analytical analysis of the bifurcation behavior of creep groan. Z. Angew. Math. Mech. (2019). https://doi.org/10.1002/zamm.201800321

[9] Neis, P.D., Ferreira, N.F., Poletto, J.C., Matozo, L.T., Masotti, D.: Quantification of brake creep groan in vehicle tests and its relation with stick-slip obtained in laboratory tests. Journal of Sound and Vibration (2016). https://doi.org/10.1016/j.jsv.2016.01.036

[10] Meng, D., Zhang, L., Xu, J., Yu, Z.: A Transient Dynamic Model of Brake Corner and Subsystems for Brake Creep Groan Analysis. Shock and Vibration (2017). https://doi.org/10.1155/2017/8020797

[11] Meng, D., Shen, L., Zhang, L., Chen, G.S.: Transient Dynamic Analysis of Vehicle Brake Creep Groan. J. Vib. Eng. Technol. (2019). https://doi.org/10.1007/s42417-019-00152-x

[12] Pürscher, M., Huemer-Kals, S., Fischer, P.: Experimental and Simulative Study of Creep Groan in Terms of MacPherson Axle Bushing Elasticities. In: EuroBrake 2018. Conference Proceedings, The Hague, 22-24 May. FISITA (2018)

[13] Huemer-Kals, S.; Pürscher, M.; Sternat, A.; Fischer, P.: Startup and Bifurcation Behavior of Non-Linear Stick-Slip Vibrations: Creep Groan Occurrence for Increasing and Decreasing Speeds. In: EuroBrake 2020. Conference Proceedings, EB2020-FBR-032. Barcelona, 2-4 June: FISITA (2020)

[14] Hase, A.: Acoustic Emissions during Tribological Processes, In: International Tribology Conference, September 16th–20th, Tokyo, Japan (2015)

[15] Ferrer, C., Salas, F., Pascual, M., Orozco, J.: Discrete acoustic emission waves during stick–slip friction between steel samples. Tribology International (2010). https://doi.org/10.1016/j.triboint.2009.02.009

[16] Stoica, N.A., Petrescu, A.M., Tudor, A., Predescu, A.: Tribological properties of the disc brake friction couple materials in the range of small and very small speeds. IOP Conference Series: Materials Science and Engineering (2017). https://doi.org/10.1088/1757-899X/174/1/012019

[17] Morissette, L., Chartier, S.: The k-means clustering technique: General considerations and implementation in Mathematica. TQMP (2013). https://doi.org/10.20982/tqmp.09.1.p015

[18] Vattani, A.: k-means Requires Exponentially Many Iterations Even in the Plane. Discrete Comput Geom (2011). https://doi.org/10.1007/s00454-011-9340-1